Mesoporous Organosilicates from Multiple Precursors: Co-Condensation or Phase Segregation/Separation?

Yong Yang and Abdelhamid Sayari*

Department of Chemistry, University of Ottawa, Ottawa, Ontario K1N 6N5, Canada

Received January 8, 2008. Revised Manuscript Received February 7, 2008

Periodic mesoporous organosilicates were synthesized under basic conditions using mixtures of phenyl and biphenyl silsesquioxane precursors in the presence of octadecyltrimethylammonium chloride as structure-directing agent. In addition to the hexagonally arranged mesopores, the materials derived from mixed precursors exhibited two distinct molecular-scale periodicities indicative of the occurrence of both phenylsilica and biphenyl silica lamellar structures within the pore walls. These data are consistent with either phase separation or island formation.

Introduction

Periodic mesoporous organic–inorganic hybrid materials with two or more organic functionalities may be prepared using different strategies depending on the location of such species, i.e., on the pore surface and/or within the pore walls.[1] Building periodic mesoporous materials with multiple organic functional groups can be achieved by different routes including (i) grafting or co-condensation of multiple organosilanes, (ii) co-condensation of an organosilane with TEOS followed by grafting a different organosilane[2] or (iii) grafting a single suitable organosilane such as propylamino- or iodosilane followed by additional synthetic steps leading to more complex surface structures such as dendrimers[3] and metal-complexed dendrimers.[4,5] Another approach is to synthesize a mesoporous organosilica with an organic spacer incorporated in the pore walls, followed by grafting an organosilane onto the pore surface, or further reactions using the organic spacer as substrate. Periodic mesoporous hybrids with both framework and surface functionalities may also be synthesized by co-condensation of an organosilsesquioxane and an organosilane.[2,6–8] Two (or conceivably more) organic functionalities may also be integrated within the pore walls using an organosilsesquioxane precursor that already contains such functionalities.[7,9,10] One more approach is to use multiple organosilsesquioxane precursors in the same synthesis. The latter method was used by several groups[11–13] to prepare periodic mesoporous organosilica (PMO) containing two or three organic spacers including phenylene, ethane, and thiophene within the pore walls. In all cases, the data have been interpreted assuming the occurrence of a single PMO mesophase with the organic spacers randomly located within the pore walls. However, the question as to whether one or more phases occurred was not specifically addressed. Indeed, all the techniques used to characterize the obtained materials, namely, XRD, NMR, TEM, Raman spectroscopy, and nitrogen adsorption, may not provide a clear-cut answer as to whether a highly dispersed multiphase system or a single mesophase with all organic spacers located randomly within the pore walls has been achieved. Recently, Treuherz and Khimyak[14] synthesized hexagonal PMO materials using ethane and ethylene-bridged silsesquioxane precursors. They used $^{1}H-^{13}C$ and $^{1}H-^{29}Si$ cross polarization MAS NMR to specifically address the issue as to whether both organic spacers are located within the same "bifunctional" mesophase or in different, highly dispersed mesophases. The cross polarization kinetics data seem to indicate that both functionalities are incorporated in the same PMO structure; however, with heterogeneous distribution of the organic spacers.

* To whom correspondence should be addressed. E-mail: abdel.sayari@uottawa.ca.

(1) (a) Brunel, D. *Microporous Mesoporous Mater.* **1999**, *27*, 329. (b) Sayari, A.; Hamoudi, S. *Chem. Mater.* **2001**, *13*, 3151. (c) Hoffmann, F.; Cornelius, M.; Morell, J.; Fröba, M. *Angew. Chem., Int. Ed.* **2006**, *45*, 3216. (d) Stein, A.; Melde, B.; Schroden, J. R. C. *Adv. Mater.* **2000**, *12*, 1403. (e) Hunks, W. J.; Ozin, G. A. *J. Mater. Chem.* **2005**, *15*, 3716. (f) Descalzo, A. B.; Jimenez, D.; Marcos, M. D.; Martinez-Manez, R.; Soto, J.; El Haskouri, J.; Guillem, C.; Beltran, D.; Amoros, P.; Borrachero, M. V. *Adv. Mater.* **2002**, *14*, 966. (g) Anwander, R.; Nagl, I.; Widenmeyer, M.; Engelhardt, G.; Groeger, O.; Palm, C.; Roeser, T. *J. Phys. Chem. B* **2000**, *104*, 3532. (h) Van Der Voort, P.; Vercaemst, C.; Schaubroeck, D.; Verpoort, F. *Phys. Chem. Chem. Phys.* **2008**, *10*, 347.

(2) Zhang, W.-H.; Lu, X.-B.; Xiu, J.-H.; Hua, Z.-L.; Zhang, L.-X.; Robertson, M.; Shi, J.-L.; Yan, D.-S.; Holmes, J. D. *Adv. Funct. Mater.* **2004**, *14*, 544.

(3) (a) Reynhardt, J. P. K.; Yang, Y.; Sayari, A.; Alper, H. *Adv. Funct. Mater.* **2005**, *15*, 1641. (b) Acosta, E. J.; Carr, C. S.; Simanek, E. E.; Shantz, D. F. *Adv. Mater.* **2004**, *16*, 985. (c) Jiang, Y.; Gao, Q. *J. Am. Chem. Soc.* **2006**, *128*, 716.

(4) Reynhardt, J. P. K.; Yang, Y.; Sayari, A.; Alper, H. *Chem. Mater.* **2004**, *16*, 4095.

(5) Reynhardt, J. P. K.; Yang, Y.; Sayari, A.; Alper, H. *Adv. Synth. Catal.* **2005**, *347*, 1379.

(6) Asefa, T.; Kruk, M.; MacLachlan, M. J.; Coombs, N.; Grondey, H.; Jaroniec, M.; Ozin, G. A. *J. Am. Chem. Soc.* **2001**, *123*, 8520.

(7) Olkhovyk, O.; Pikus, S.; Jaroniec, M. *J. Mater. Chem.* **2005**, *15*, 1517.

(8) Alauzun, J.; Mehdi, A.; Reyé, C.; Corriu, R. J. P. *J. Am. Chem. Soc.* **2006**, *128*, 8718.

(9) Cornelius, M.; Hoffmann, F.; Fröba, M. *Chem. Mater.* **2005**, *17*, 6674.

(10) Sayari, A.; Wang, W. *J. Am. Chem. Soc.* **2005**, *127*, 12194.

(11) Burleigh, M. C.; Jayasundera, S.; Spector, M. S.; Thomas, C. W.; Markowitz, M. A.; Gaber, B. P. *Chem. Mater.* **2004**, *16*, 3.

(12) Morell, J.; Güngerich, M.; Wolter, G.; Jiao, J.; Hunger, M.; Klar, P. J.; Fröba, M. *J. Mater. Chem.* **2006**, *16*, 2809.

(13) Cho, E.-B.; Kim, D.; Jaroniec, M. *Langmuir* **2007**, *23*, 11844.

(14) Treuherz, B. A.; Khimyak, Y. Z. *Microporous Mesoporous Mater.* **2007**, *106*, 236.

10.1021/cm800069u CCC: $40.75
Published on Web 04/15/2008

In the current work, mesoporous materials using mixtures of phenyl and biphenyl-silsesquioxanes were prepared under basic conditions where, in addition to the long-range order of the pore system, molecular order within the pore walls is expected to occur.[15,16] Under such conditions, the one- or two-phase issue may be delineated.

Experimental Section

Materials. The two-precursor derived PMO materials were synthesized using mixtures with different molar ratios of 1,4-bis(triethoxysilyl)benzene (BTEB) and 4,4′-bis(triethoxysilyl)-1,1′-biphenyl (BTEBP) in the presence of octadecyltrimethylammonium chloride (ODTMA) as structure-directing agent under basic conditions. Typically, 0.835 g (2.4 mmol) of ODTMA was dissolved in a mixture of 25.16 g of distilled water and 0.40 g (10 mmol) of NaOH at 35 °C. The required amount of BTEB and BTEBP mixture (2.5 mmol in total) was added to the ODTMA solution under vigorous stirring. The stirring was maintained overnight, then the mixture was transferred into a Teflon-lined autoclave and heated at 100 °C for 20 h. The resulting white precipitate was recovered by filtration and dried to yield as-made PMO material. The surfactant was removed by stirring 1.0 g of as-made material in 150 mL of ethanol and 5 g of concentrated HCl aqueous solution at room temperature for 5 h. This procedure was carried out twice.

Methods. X-ray diffraction patterns of all samples were recorded using a Philips X'pert instrument equipped with a solid-state detector using Cu Kα radiation with 0.15418 nm wavelength, a step size of 0.02° 2θ, and a counting time per step of 4.0 s over a $1.4° < 2\theta < 50°$ range. Nitrogen adsorption experiments were performed at 77 K using a Coulter Omnisorp 100 gas analyzer. Samples were evacuated at 50 °C for several hours to remove the surface humidity and preadsorbed gases before exposure to nitrogen. The specific surface area, S_{BET}, was determined from the linear part of the BET plot ($P/P_0 = 0.05$–0.15). The average pore size was the peak value on the pore size distribution (PSD), which was calculated from the adsorption branch using the KJS (Kruk, Jaroniec, Sayari) method.[17] The total pore volume, V_t, was determined from the amount of liquid N_2 adsorbed at a relative pressure of about 0.99. Transmission electron micrographs (TEM) were obtained using a JEOL 2100F operated at 200 kV. Before examination, the specimen were dispersed in anhydrous ethanol and deposited on a holey carbon film on a copper grid. ^{29}Si and ^{13}C CP MAS NMR spectra were collected at room temperature on a Bruker ASX200 instrument in a magnetic field of 4.7 T (the resonance frequencies were 50.3 and 39.7 MHz, respectively). Thermal decomposition of the materials was performed using a TA Instruments Q500 thermogravimetric analyzer from room temperature to 900 °C under flowing nitrogen, and then to 1000 °C under air with a heating rate of 10 °C/min. Raman spectra of the materials were collected with a HORIBA Jobin Yvon LabRam-IR HR800 instrument. The powdered samples were irradiated with a Ar-ion laser light ($\lambda = 514.532$ nm), and the backscattered radiation was collected through a 100× objective lens with a 0.9 numerical aperture, a specific notch filter for the rejection of the exciting line, a 200 μm spectrograph entrance slit, and then detected by a CCD camera. A grating with 1800 grooves per mm was used for high-resolution measurements. The spectra were acquired for a 400−1800 cm^{-1} range with an integration time of 10 cycles by 5 s each.

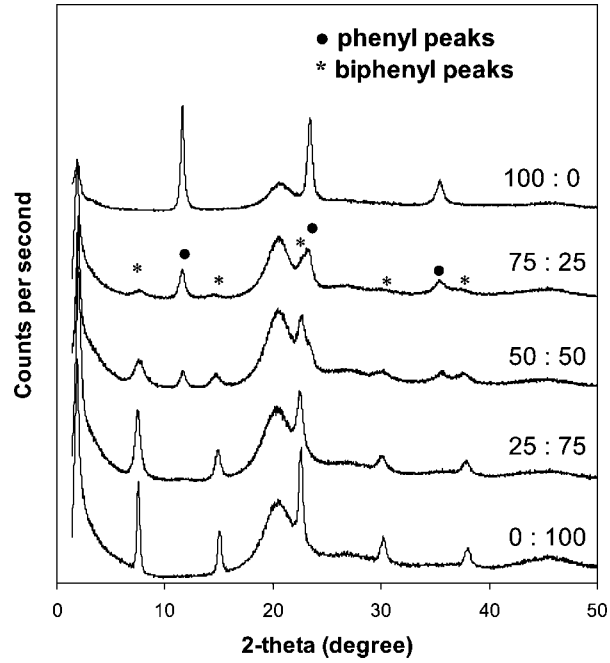

Figure 1. Powder X-ray diffraction profiles of phenylene/biphenylene-bridged mesoporous organosilicas. The BTEB : BTEBP molar ratios used in the synthesis mixture are shown on the right-hand side.

Results and Discussion

The XRD patterns of the surfactant-free PMO materials synthesized using different molar ratios of BTEB and BTEBP precursors are shown in Figure 1. All samples exhibited a single intense peak at ~2.0° 2θ attributable to the occurrence of a mesophase. The corresponding *d*-spacing was about 44 Å regardless of the gel composition. No additional peaks attributable to the mesophase structure were detected. However, a series of regularly spaced diffraction peaks was also obtained. For the pure biphenylene-bridged PMO, these peaks appeared at *d*-spacings of 11.6, 5.9, 3.9, 2.9, and 2.4 Å. They were assigned to a lamellar structure within the pore walls with a d_{001} spacing of 11.6 Å, consistent with the length of the O−Si−C_6H_4−C_6H_4−Si−O units.[16,18] Similarly, pure phenylene-bridged organosilica exhibited a series of diffraction peaks at *d*-spacings of 7.6, 3.8, and 2.5 Å. These peaks also stem from the molecular-scale ordering of the organic spacer into a layered structure within the pore walls.[15] As seen in Figure 1, with increasing BTEB:BTEBP ratios in the synthesis mixture, the relative intensity of the peaks corresponding to the molecular-scale periodicity of both types of bridging groups changed accordingly. Notice that in most of earlier reports,[11–13] multiple-precursor PMOs were synthesized in the presence of nonionic surfactants under acidic conditions where molecular-scale order is difficult to achieve.[19]

Transmission electron microscopy image of the material prepared using an equimolar mixture of BTEB and BTEBP

(15) (a) Inagaki, S.; Guan, S.; Ohsuna, T.; Terasaki, O. *Nature* **2002**, *416*, 30. (b) Yang, Q.; Kapoor, M. P.; Inagaki, S. *J. Am. Chem. Soc.* **2002**, *124*, 9694.
(16) Kapoor, M. P.; Yang, Q.; Inagaki, S. *J. Am. Chem. Soc.* **2002**, *124*, 15176.
(17) Kruk, M.; Jaroniec, M.; Sayari, A. *Langmuir* **1997**, *13*, 6267.
(18) Yang, Y.; Sayari, A. *Chem. Mater.* **2007**, *19*, 4117.
(19) Goto, Y.; Okamoto, K.; Inagaki, S. *Bull. Chem. Soc. Jpn.* **2005**, *78*, 932.

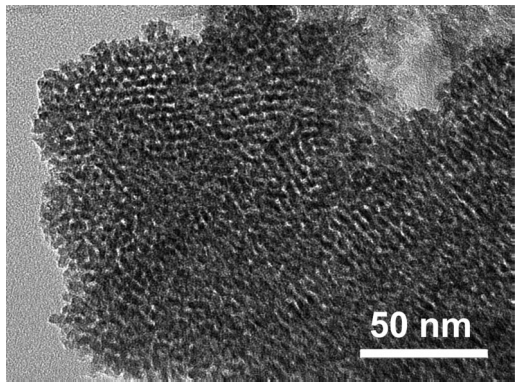

Figure 2. Transmission electron microscopy (TEM) image of the PMO prepared in the presence of a BTEB−BTEBP equimolar mixture.

shown in Figure 2 clearly indicates the formation of an ordered mesostructure with a hexagonal arrangement of mesoporous channels.

Nitrogen adsorption–desorption isotherms and the corresponding pore size distributions are shown in Figure 3. All isotherms exhibited a step increase at $P/P_0 = 0.2-0.5$ attributable to the condensation of nitrogen in mesopores with relatively narrow size distributions. As shown in Figure 3B, the average pore size ranged from 3.2 nm for pure biphenylene-bridged PMO to 3.7 nm for pure phenylene-bridged PMO. The structural properties of all samples as derived from XRD and nitrogen adsorption measurements are listed in Table 1. As can be seen, the BET surface area was in the range of 365–592 m^2/g with no clear relationship with the BTEB:BTEBP ratio used in the synthesis.

Solid-state ^{13}C and ^{29}Si NMR measurements of the solvent-extracted PMOs were carried out to verify the occurrence of covalent C−Si bond and the organic spacers within the pore walls of PMOs. As shown in Figure 4A, the ^{13}C CP MAS NMR spectra of the pure biphenylene-bridged material exhibited four distinct peaks with chemical shifts of 125.5, 130.4, 134.0, and 141.2 ppm attributable to the four different carbons in the biphenyl ring.[16,18] With increasing amounts of BTEB in the synthesis mixture, a new peak at 133.0 ppm developed gradually. This peak was assigned to the four identical carbon atoms in the benzene ring.[15] The two peaks at ∼210 and ∼58 ppm in the pure benzene-bridged PMO spectrum are side bands.[11,15] The ^{29}Si MAS NMR spectrum of biphenylene-bridged PMO featured three signals at −61.5, −71, and −81.0 ppm, which were attributed to T^1 [C*Si*(O-Si)$(OH)_2$], T^2 [C*Si*$(OSi)_2OH$,] and T^3 [C*Si*$(OSi)_3$] silicon resonances, respectively.[16] No major changes occurred in the shape of ^{29}Si NMR signal as a function of BTEB:BTEBP ratio. However, the relative intensity of T^3 increased significantly at the expense of T^1 indicating that the BTEB-derived PMO exhibits a higher degree of condensation than its BTEBP counterpart. No Q^n [*Si*$(OSi)_n(OH)_{4-n}$] species were detected in the range −90 to −110 ppm indicating that no separate silica phase occurred, and all the Si−C bonds were preserved during the material synthesis and surfactant removal.

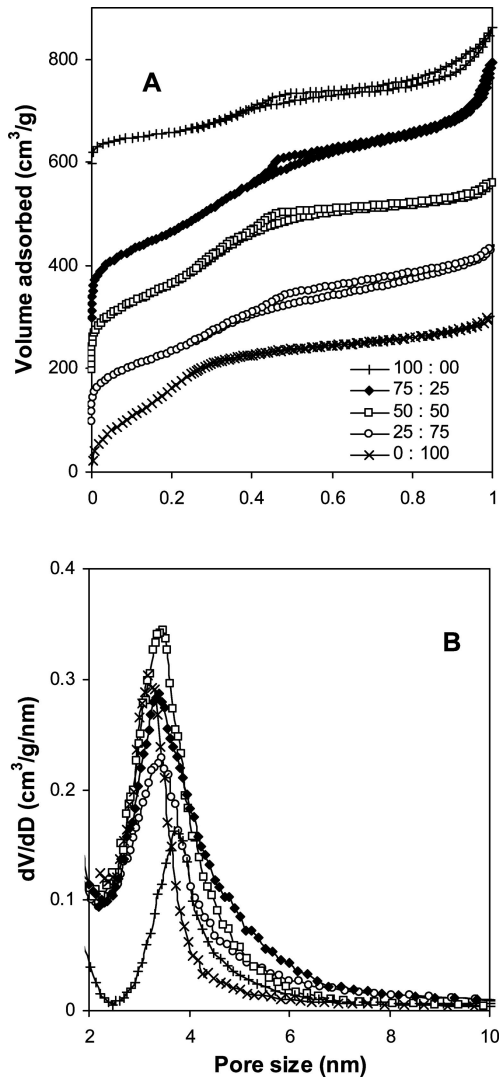

Figure 3. (A) Nitrogen adsorption–desorption isotherms and (B) the corresponding pore size distributions of phenylene/biphenylene-bridged mesoporous organosilicas. The BTEB : BTEBP molar ratios used in the synthesis mixture are shown on the right-hand side.

Raman spectroscopy was used to further verify the occurrence of phenylene and biphenylene rings in the framework of the solvent-extracted PMOs. As shown in Figure 5, the peaks attributable to biphenyl species, i.e., biphenyl interring stretching (ν-ring at 1602−1606 cm^{-1}), biphenyl rings δ(C−H) at 1520 cm^{-1} and C−C stretching at 1285 cm^{-1}, C−H bending in plane rings at 1137 cm^{-1} and C−H bending out of plane rings at 798 cm^{-1} are clearly observed.[18,20–22] Increasing the amount of BTEB in the synthesis mixture gave rise to a new peak at 1104 cm^{-1}, which can be attributed to the phenyl ring breathing mode. This peak increased significantly in the pure phenylene-bridged sample. In addition, two other bands were also observed which can be attributed to the phenyl species, i.e., phenylene ν-ring at 1598 cm^{-1} and δ-ring at 636 cm^{-1}. The origin of the band at 783 cm^{-1}, which appear for BTEB-containing materials, is uncertain.[20]

(20) Hoffmann, F.; Güngerich, M.; Klar, P. J.; Fröba, M. *J. Phys. Chem. C* **2007**, *111*, 5648.
(21) Yu, K. H.; Rhee, J. M.; Lee, Y.; Lee, K.; Yu, S.-C. *Langmuir* **2001**, *17*, 52.
(22) Lee, C. W.; Pan, D.; Shoute, L. C.; Phillips, D. L. *Res. Chem. Intermed.* **2001**, *27*, 485.

Table 1. Physicochemical Properties of Mesoporous Organosilicas

sample	BTEB: BTEBP	d_{100} (nm)	surface area (m^2/g)	pore size (nm)	pore volume (cm^3/g)	wall thickness (nm)	calcd weight loss[a] (wt %)	TGA weight loss (wt %) raw data[b]	TGA weight loss (wt %) corrected[c]
S-1	100:0	4.68	365	3.7	0.48	1.76	42.2	38.5	46.7
S-2	75:25	4.62	473	3.4	0.77	1.93	46.4	41.0	48.9
S-3	50:50	4.59	586	3.4	0.56	1.90	50.6	47.5	55.5
S-4	25:75	4.48	592	3.4	0.53	1.78	54.7	52.5	58.8
S-5	0:100	4.55	480	3.2	0.46	2.10	58.9	59.5	64.9

[a] Calculated on the basis of the formula $xO_{1.5}SiC_6H_4SiO_{1.5} + (1-x)O_{1.5}SiC_{12}H_8SiO_{1.5}$, where x is the molar percentage of BTEB in the synthesis mixture, i.e., $x = M_{BTEB}/(M_{BTEB} + M_{BTEBP})$. [b] Apparent weight loss obtained directly from the TGA profile. [c] The final weight of SiO_2 was corrected to the corresponding weight of "Si_2O_3" so that the corrected TGA weight loss (column 10) would have the same definition as the calculated weight loss (column 8).

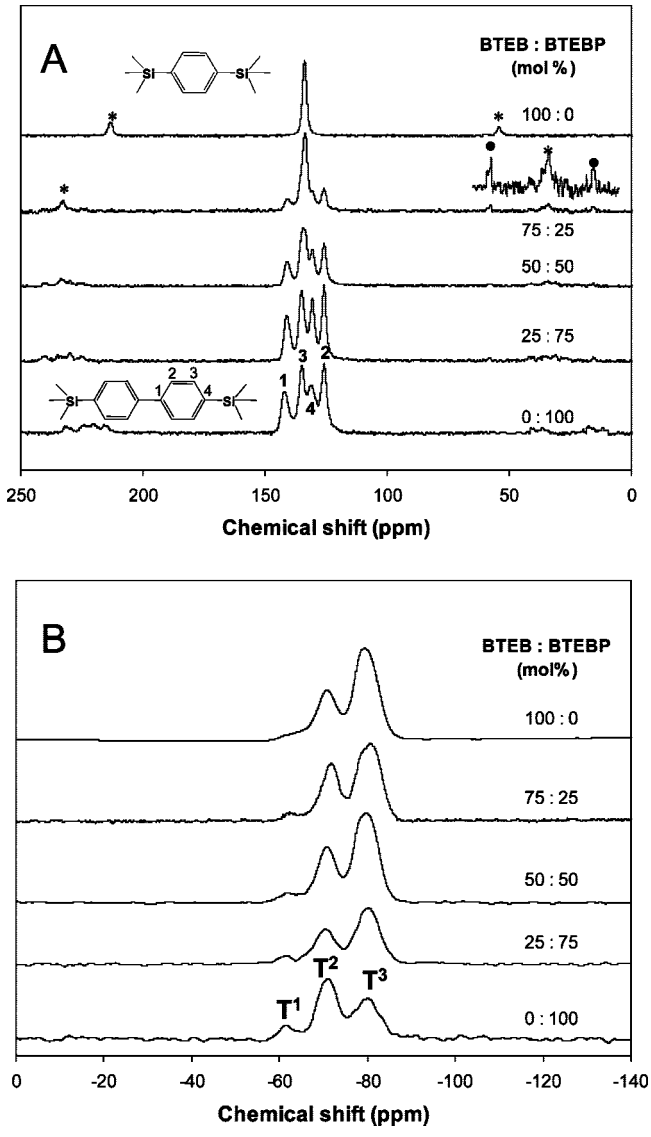

Figure 4. ^{13}C CP-MAS and ^{29}Si MAS NMR spectra of extracted phenylene/biphenylene-bridged mesoporous organosilicas. The BTEB : BTEBP molar ratios used in the synthesis mixture are shown on the right-hand side. (*) side bands, (●) ethoxy groups.

All TGA profiles were similar to each other. The decomposition of the materials started at 480−500 °C and reached a maximum between 650 and 750 °C depending on the material. At the end of the first stage carried out under nitrogen between room temperature and 900 °C, the weight loss was ca. 10–15%, indicating that most of the organic materials were released only when the gas flow was switched to air.

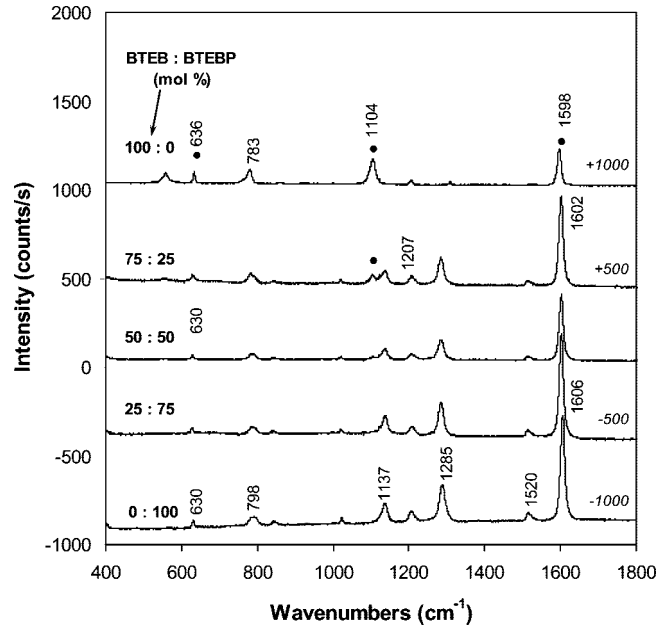

Figure 5. Laser Raman spectra of extracted phenylene/biphenyl-bridged organosilicas. The peaks with "●" belong to phenyl species. Spectra were shifted upward or downward by the amounts shown on the right-hand side.

The TGA data shown in Table 1 lend further support to the contention that both precursors contributed to the formation of the final material in the same ratio as in the original synthesis mixture. The weight loss calculated on the basis of the gel composition and assuming that the final product is "Si_2O_3" is shown in column 8 (Table 1). To be compared to the calculated weight loss, the TGA raw data (Table 1, column 9) should be corrected taking into account that in the TGA experiment, the final product was SiO_2, not "Si_2O_3". The corrected weight loss data are shown in column 10 (Table 1). As seen, the corrected TGA weight loss was 5−10% higher than the calculated weight loss. This is due to some non hydrolyzed ethoxy groups as seen in the ^{13}C CP-MAS NMR spectra (Figure 4A). On the basis of data in columns 8 and 10 (Table 1), it can be demonstrated that fewer than one in ten ethoxy groups did not hydrolyze.

Figure 6 shows SEM images for representative phenylene/biphenylene-containing mesoporous organosilica samples. The morphology changed when changing the relative amount of the two precursors. Pure mesoporous phenylene and biphenylene-bridged silica exhibited quite different morphologies. The pure phenylene-silica consisted of fibers aggregated into large particles, whereas the pure biphenylene-

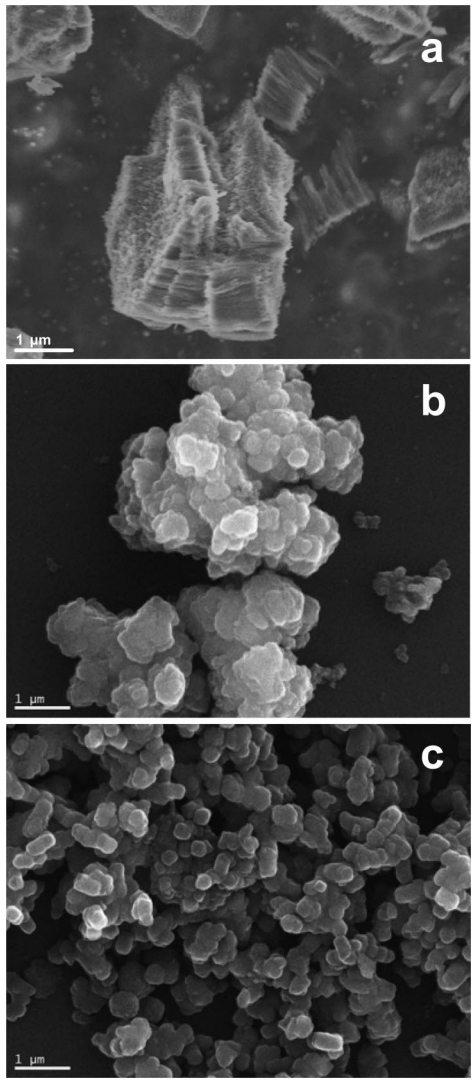

Figure 6. SEM images of extracted organosilicas: (a) pure phenylene-bridged PMO, (b) PMO from BTEB-BTEBP equimolar mixture, and (c) pure biphenylene-bridged PMO. All images were collected under the same magnification, 10 000×.

silica comprised uniform particles less than 1 μm in length. The material derived from an equimolar mixture of BTEB and BTEBP (Figure 6b) comprised agglomerated submicron particles with irregular shapes.

With the exception of XRD data, all other findings may be interpreted on the basis of a single PMO mesophase containing both phenylene and biphenylene spacers. Raman and NMR data indicate that both spacers occur in the materials, whereas TGA measurements are consistent with the occurrence of both species in the same ratio as in the synthesis gel. However, none of these techniques discriminates between a single-phase PMO and a highly dispersed mixture of two PMOs. Because of the fact that the pore sizes and unit-cell dimension of both phenylene and biphenylene-bridged PMOs are very close, it is difficult to detect for example a bimodal pore size distribution in mixed-precursor materials (by TEM or nitrogen adsorption) or two well-resolved d_{100} diffraction peaks. Also, SEM images did not show for example particles with different morphologies in mixed-precursor materials that would be associated with separate PMO mesophases. Moreover, EDX mapping failed to identify distinct areas with different carbon to silicon ratios. However, under our synthesis conditions, the occurrence of two distinct molecular-scale orders associated with phenylene and biphenylene species as shown by XRD is inconsistent with the formation of a single PMO mesophase with randomly distributed organic spacers. Our XRD data indicate that either phase separation or segregation took place. In the former case, separate yet highly dispersed phenylene and biphenylene PMO mesophases are formed, whereas in the latter case, islands of different PMOs are formed within the same particles. In both cases, the size of single spacer PMO domains should be large enough for well-resolved diffraction patterns to occur.

This work shows that using multiple silsesquioxane precursors does not necessarily give rise to single-phase PMOs with all organic spacers randomly distributed within the pore wall. Phase separation or phase segregation (i.e., island formation) may occur.

Acknowledgment. The generous financial support of the Natural Sciences and Engineering Council of Canada (NSERC) and the Ontario Research & Development Challenge Fund (ORDCF) is acknowledged. A.S. thanks the Canadian Government for a Canada Research Chair in Catalysis by Nanostructured Materials (2001–2008).

CM800069U